AD-A120 582 HIGH-CURRENT PULSED ELECTRON ACCELERATOR(U) FOREIGN TECHNOLOGY DIV WRIGHT-PATTERSON AFB OH 28 JUL 82 FTD-ID(RS)T-1718-81 1/1

UNCLASSIFIED F/G 20/7 NL

END

FILMED

DTIC

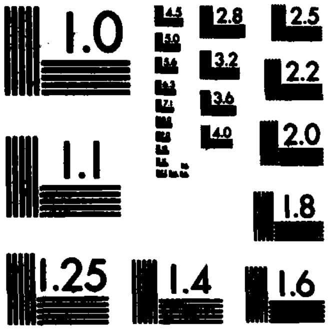

MICROCOPY RESOLUTION TEST CHART
NATIONAL BUREAU OF STANDARDS-1963-A

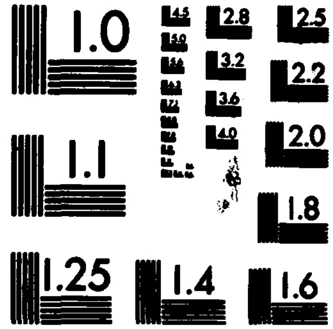

MICROCOPY RESOLUTION TEST CHART
NATIONAL BUREAU OF STANDARDS-1963-A

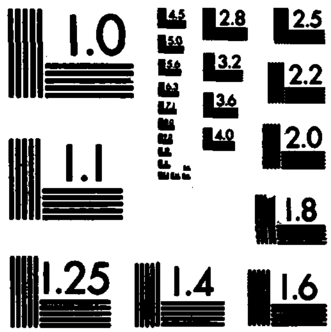

MICROCOPY RESOLUTION TEST CHART
NATIONAL BUREAU OF STANDARDS-1963-A

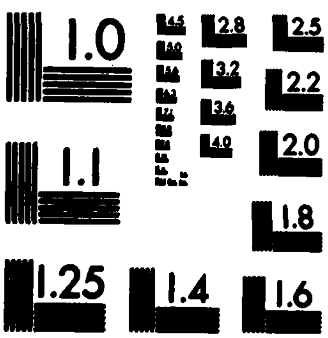

MICROCOPY RESOLUTION TEST CHART
NATIONAL BUREAU OF STANDARDS-1963-A

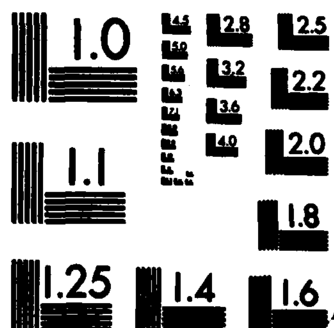

MICROCOPY RESOLUTION TEST CHART
NATIONAL BUREAU OF STANDARDS-1963-A

FTD-ID(RS)T-1718-81

AD A120582

FOREIGN TECHNOLOGY DIVISION

VI.. HIGH-CURRENT PULSED ELECTRON ACCELERATOR

Approved for public release;
distribution unlimited.

EDITED TRANSLATION

FTD-ID(RS)T-1718-81 28 July 1982

MICROFICHE NR: FTD-82-C-001031

~~VI~~ HIGH-CURRENT PULSED ELECTRON ACCELERATOR

English pages: 9

Source: Institute of Atomic Energy Annual Report, 1979, pp. 58-62

Country of origin: China
Translated by: Randy Dorsey
Requester: FTD/TQTD

PREPARED BY:

TRANSLATION DIVISION
FOREIGN TECHNOLOGY DIVISION
WP-AFB, OHIO.

GRAPHICS DISCLAIMER

All figures, graphics, tables, equations, etc. merged into this translation were extracted from the best quality copy available.

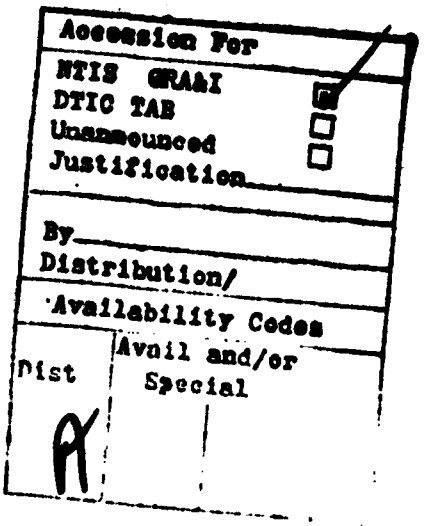

VI. HIGH-CURRENT PULSED ELECTRON ACCELERATOR

1. Physical layout and engineering design of high-current pulsed electron accelerator

(Charged Particle Inertial Confinement Research Group)

The principal criteria for the high-current pulsed electron accelerator are as follows:

Electron energy	1 MeV
Electron beam current	80 kA
Pulse duration	70 ns
Beam current energy	5.6 kJ
Beam current power	8×10^{10} W

When the electron beam focal spot diameter $\sim$1.5mm, the beam current power density is $4.53 + 10^{12}$ W/cm^2. The accelerator configuration is shown in Fig. 1.

The main parameters of the high-current pulsed electron accelerator are as follows:

(1) Impulse voltage generator:

Total inductance L_m	15 μH
Output capacitance C_m	35 nF
Impulse voltage generator to transmission line charging frequency ω	2.013×10^6/s

(2) Water-medium double-layer coaxial transmission line:

Maximum charging voltage	1.12MV and 1.21MV
Inner line impedance	4.217 Ω

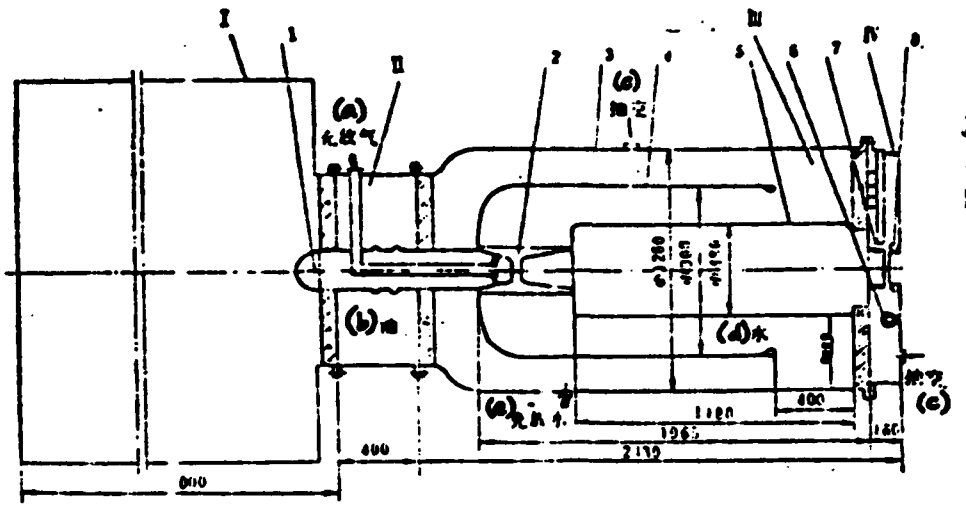

Fig. 1. High-current pulsed electron accelerator configuration

KEY: 1. Wiring board; 2. Main switch; 3. Outer cylinder; 4. Intermediate cylinder; 5. Inner cylinder; 6. Integrating loop; 7. Prepulse switch; 8. Rogowski coil; I. Marx generator; II. Transition chamber; III. Transmission line; IV. Diode; (a) gas charging and release; (b) oil; (c) air evacuation; (d) water; (e) water fill and drain.

Outer line impedance	2.17Ω
Transition stage impedance	6.474Ω
Inner line capacitance	8.48 nF
Outer line capacitance	22.6 nF
Transmission line electrical length	70 ns
Outside diameter of inner cylinder	48 cm
Inside diameter of intermediate cylinder	90 cm
Outside diameter of intermediate cylinder	91 cm
Inside diameter of outer cylinder	126 cm

(3) Main Switch:

Electrode separation	~2 cm
Maximum electric field inside main switch	0.54 MV/cm
Main switch inductance	~14.9 nH

(4) Diode:

Diode impedance	~6Ω
Diode capacitance	~32.9 nF
Diode inductance	~35.5 nH
Electron beam rise time	~25 ns

1. Impulse voltage generator. It consists of twenty 0.7 μF capacitors. When charging voltage is 70 kW the impulse voltage generator stored energy is 34.3 kJ and its output capacitance is 35 nF. It employs plus-minus dc power source charging. There are 10 ball gaps. The capacitors, ball gaps, charge resistors, and ground resistors are all submerged in a large oil tank filled with approximately 30 tons of transformer oil.

A schematic diagram of the impulse voltage generator is shown in Figure 2. The first and second ball gaps employ the external triggering method. The third pair to the tenth pair of ball gaps depend on overvoltage to cause their successive breakdown.

The total inductance of the impulse voltage generator is 14.3 μH, of which connector wire inductance is 8.83 μH. The impulse voltage generator to transmission line charging time is approximately 0.9 μs. Reducing the inductance of the impulse voltage generator as much as possible will, in turn, reduce the charging time of the transmission line, reduce the transmission line voltage hold-off capability and reduce the leakage energy of the water medium in the transmission line (water medium leakage time constant is 7 μs). Improving the quality of the pulse capacitor reduces its bulk and thereby reduces on-line inductance, which is an important step in decreasing impulse voltage generator inductance. The overvoltage values of the various ball gaps were calculated using resistance grid simulation.

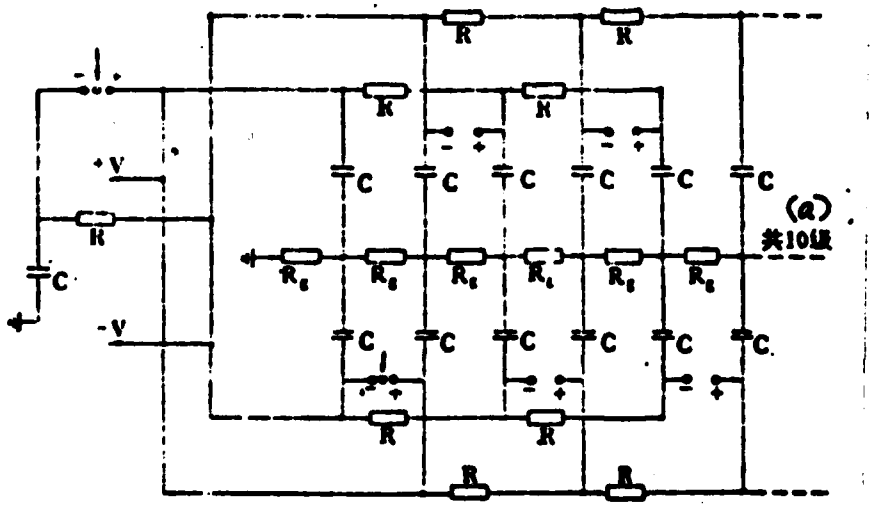

Fig. 2. Schematic diagram of impulse voltage generator
KEY: (a) 10 stages in all.

2. Water-medium double-layer coaxial transmission line. Resonant charging of the double-layer coaxial transmission line by the impulse voltage generator was used to increase energy transmission efficiency. In the physical layout of the accelerator, numerical solutions of Laplace transformations and numerical solutions of equations of state on a computer were used to quite accurately obtain voltage transmission and energy transmission efficiency, respectively.

Taking into account the insulation hold-off and geometric dimensions of the transmission line, in order to ensure that the actual field strengths of the different points inside the transmission line are all less than the permissible field strength and still have an ample safety coefficient, the diameter of the inner, intermediate, and outer cylinders of the transmission line were selected primarily on the basis of the formula of electrical breakdown in the water medium[1] (see the K values in Table 1). Combining voltage hold-off and voltage transmission requirements and energy transmission requirements we carried out calculations of optimum parameters on a computer.

	(a) MV	(b) cm^3	(c) kV/cm	(d) kV/cm	$K = \frac{E}{F}$
(e)	0.09	17300	80.2	141.2	0.568
(f)	-1.12	46800	42.7	257.2	0.166
(g)	-1.12	47500	76	257.6	0.295
(h)	0	72400	55	125	0.44
(i)		5330	108	314	0.344

Table 1. Electrical field parameters of Blumlein transmission line arrangement

* The values of permissible field strength F are based on the J. C. Martin formula and calculations are obtained with the effective charging time $t_{eff} = 0.6$ μs.

KEY: (a) Charging voltage; (b) Electrode area; (c) Experimental field strength; (d) Permissible field strength; (e) Outer surface of inner cylinder; (f) Inner surface of intermediate cylinder; (g) Outer surface of intermediate cylinder; (h) Inner surface of outer cylinder; (i) At the tip of intermediate cylinder.

The principal field strength parameters in the design of the transmission line are listed in the table. The field strengths of the

transmission line were calculated on a TQ-6 electronic computer using the grid method. Particular emphasis was given to the investigation of electric field distribution at the tip of the intermediate cylinder and at the head of the outer cylinder. The tip of the intermediate cylinder and the head of the outer cylinder were refined and shaped into a reasonable arrangement, thereby improving the voltage hold-off ability of the transmission line.

The transmission line intermediate cylinder employs rutile ceramic which has a dielectric constant ε = 75-80. Experiments have determined that its voltage hold-off is 12kV/mm for a carrier pulse in water at a rise time of 2 μs and since its dielectric constant (81) is relatively close to that of water, it can reduce the effect which the support member has on electric magnetic propagation in the water.

Under short pulse, high voltage conditions, water is a fairly ideal transmission line medium. Deionization treatment is conducted on the water, ensuring that the resistivity of the water is greater than 1MΩcm. The deionized water system provides 0.5 tons of water per hour. During the process of filling the transmission line with water, in order to prevent the air inside the transmission line from getting into the water and forming bubbles which are likely to give rise to electrical breakdown, steps are taken to extract the air from the transmission line before it is filled with water.

3. Ball gap and main switch. The material of the outer sleeve of the spark ball gap is Nylon-6 and its outside diameter is 150mm, the inside diameter is 110mm, and the length is 300mm. The shape of the ball gap electrodes is designed primarily to ensure that the center portion in the ball gap is a uniform electric field region[2], and therefore the head of the both electrodes must have a flattened section. Calculations were made on a TQ-6 computer of the electric field conditions under conditions of various diameters of the flattened sections as well as curvature radii of transition from the flattened head to the rear base of the electrodes. Stainless steel or copper-tungsten alloy was employed for the electrode material of the ball gap heads. The ball gaps were filled with N_2 or a gas mixture (90% N_2 and 10% SF_6) at 1 - 4 atmospheres and dependence curves were

constructed for breakdown voltage and inflation pressure at different electrode separation distances.

In order to reduce the inductance of the main switch, it was filled with SF_6 gas at 10 atmospheres and the distance between electrodes was reduced.

4. Diode. The electrode impedance was designed to be 6Ω, and since the impedance of the transmission line is 6.47Ω, from the viewpoint of energy transmission efficiency, a diode impedance of 6Ω is ideal. Taking into consideration that electron beam self-pinching requires a high ν/γ value, this is even better. Optimum diode impedance can be lowered to the matching impedance. This can be achieved by changing the distance between the cathode and the anode. Simulation tests were done with several shapes and structures of diode cathodes, including needle-shaped cathodes, solid cone cathodes and hollow cone cathodes. The materials selected for use were tungsten, graphite, brass, and stainless steel. Anode material and thickness will be determined by future test objectives. At present the design employs aluminum sheet 2 - 6mm thick for conducting shakedown tests.

The diode employs a radial insulation arrangement and uses an 8cm thick organic glass plate to separate the deionized water and the vacuum region. The outside diameter of the insulation board was selected as 2.72 times its inside diameter. The field strength to which the insulation board is subjected on its inside diameter reaches a maximum value of 45kV/cm. This is much lower than the hold-off strength of organic glass already in operation which has been reported in literature. From the standpoint of voltage hold-off, we think it is reliable.

In order to control the effect of the prepulse on the diode, a section of organic glass is inserted into the cathode guide bar. Its length can vary and the size of the prepulse can be regulated by means of capacitive voltage dividing and when the main pulse arrives, due to surface discharge it passes through the inserted organic glass section.

Calculation of the electric field distribution and the electron orbits were done by computer.

5. Physical measurement of electron beam parameters. A resistive voltage divider and a capacitive voltage divider were designed for measuring the pulsed high voltage at the diode, the transmission line and the output of the impulse voltage generator. At the same time, a Rogowski coil, an integrating loop, and a current divider were designed and refined for measuring diode current and return current.

A miniature transmission line was designed and used for graduation testing of the above-mentioned current and voltage measuring equipment.

Various components of the accelerator are just now being refined.

(Written by Wang Naiyan)

Bibliography

[1] J.D.Shipman, IEEE Transaction on nuclear science, NS-16, No.4, p.243.
[2] K.R.Prestwich and D.L.Johnson, IEEE Transaction on nuclear science, NS-16, No.3, p.64.

2. Electric field calculations of a Blumlein transmission line

(by Gong (illegible), Yang Dawei, Wang Shumao, and Wang Naiyan)

The basic method of electric field calculation was the square grid super relaxation iteration method. The difference formula of the Laplace equation was employed in axisymmetric cylindrical coordinates and iterative solutions were performed at the points required by the grid matrix. Iteration was accomplished on a 129 X 561 grid matrix. A method similar to that of J. E. Boers[1] was employed in the treatment of the difference equations at the surfaces of different intermediate planes. We made derivations of the difference equations at the intersection points of the different intermediate planes.

Calculations were carried out on a TQ-6 computer using a program developed with BCY language. The program is able to directly yield the coordinate values of the equipotential lines. The equipotential lines are defined as an interval based on 5% of the electrical potential difference between the two electrodes. The program is also able to directly utilize a wide column output to machine draw an equipotential line distribution diagram. It can also draw an enlarged equipotential line distribution diagram of some areas of interest to us.

The calculation results make it clear that when the effect of the main switch is not considered, the field strength of the intermediate cylinder is representative of the maximum electric field strength in the entire area. We selected a different shaped tip which caused the electric field strength at the point in question to drop from the original 177kV/cm to approximately 108kV/cm. The electric field distribution of the entire area (without the main switch) is shown in the figure.

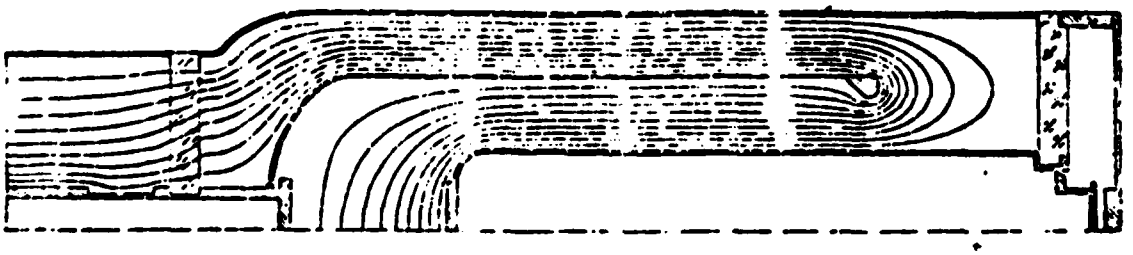

Entire area electric field distribution diagram

Bibliography

[1] J.E.Boers, Record of the 11th symposium on electron, ion and laser beam technology boulder, Colorado, 12-14 May, 1971, p.167.